Drying process of pullulan edible films forming solutions studied by low-field NMR

Qian Xiao [a,b,*], Loong-Tak Lim [b], Yujia Zhou [a], Zhengtao Zhao [b]

[a] School of Food Science and Technology, Hunan Agricultural University, Hunan 410128, China
[b] Department of Food Science, University of Guelph, N1G 2W1 Ontario, Canada

ARTICLE INFO

ABSTRACT

The dynamics of water in pullulan film-forming solutions during drying were investigated by low-field nuclear magnetic resonance. At the begin of drying, two transverse relaxation times (T_2) at around 32.77 and 2149 ms were attributed to bound and free waters in pullulan samples, respectively. An additional T_2 value, ascribed to the tightly bound water in entanglement zones of pullulan chains, appeared at around 3.51 ms as the drying process continued (beyond 1080 min of drying time). The observed three relaxation times revealed the multi-exponential relaxation behavior of water in pullulan. Moreover, the polymer exhibited spatial heterogeneity with increasing drying time from 1200 to 1920 min. On the basis of diffusive and chemical exchange model, the dimension range of pullulan network decreased from 7.69–32.66 to 4.73–18.14 μm as the pullulan films solidified. Furthermore, the rate of chemical exchange between water and pullulan significantly increased at the later stage of drying process.

© 2017 Elsevier Ltd. All rights reserved.

1. Introduction

Pullulan is an extracellular and water-soluble microbial polysaccharide produced by *Aureobasidium pullulans* in starch and sugar cultures. The linear polymer mainly consists of maltotriose units interconnected to each other by α-(1, 6) glycosidic bonds (Cheng, Demirci, & Catchmark, 2011). This unique linkage pattern endows pullulan with distinctive physical properties to form film that is strong, transparent, has low permeability to oil and oxygen, and yet water soluble (Singh, Saini, & Kennedy, 2008). Previously, we investigated the molecular networks, chain relaxation, water-pullulan/pullulan-pullulan interactions, macromolecular order and conformational change of pullulan solutions during drying. At the initial stage of drying, the interactions between pullulan molecular chains in diluted solution are minimal. However, as the drying process continues, pullulan chains interact to form an entangled network, with concomitant development of long-range relaxation as evidenced from the discrete relaxation spectra (Xiao, Tong, & Lim, 2012; Xiao, Tong, Zhou, & Deng, 2015). During drying, the oxygen atoms at the C5 and C6 carbons of the D-glucopyranose ring preferentially hydrogen bond with water or pullulan molecules, forming more-ordered structure with increased inter-chain interactions (Xiao, Tong, & Lim, 2014). Although the dynamic interactions between pullulan chains during drying have been studied, information related to the molecular mobility is currently not available.

Low-field nuclear magnetic resonance (LF NMR) spectroscopy is a non-destructive technique that can provide useful information about water at the molecular level, as the resonance phenomenon is uniquely sensitive to both local chemical and dynamic effects (Ibbett, Schuster, & Fasching, 2008). Specifically, low-resolution proton transverse relaxation time (T_2) has been used by many researchers in the investigation of the dynamics of water molecules and their distribution in a number of biopolymer and synthetic polymer systems, including pullulan, rice starch, carrageenan, aggrecan, gelatin, regenerated cellulosic fibers, Mozzarella di Bufala Campana cheese, poly(vinyl methyl ether), poly (hydroxymethyl methacrylate), and polyvinyl alcohol (Chen, Tian,

Tong, Zhang, & Jin, 2017; Foster, Damion, Baboolal, Smye, & Ries, 2016; Ghi, Hill, & Whittaker, 2002; Ghoshal, Denner, Stapf, & Mattea, 2012; Ghoshal, Mattea, Denner, & Stapf, 2010; Gianferri, D'Aiuto, Curini, Delfini, & Brosio, 2007; Ibbett et al., 2008; Okada, Matsukawa, & Watanabe, 2002; Ritota, Gianferri, Bucci, & Brosio, 2008; Spěváček, Hanyková, & Labuta, 2011; Tang, Godward, & Hills, 2000; Zhang, Matsukawa, & Watanabe, 2004).

In heterogeneous biopolymer systems, the transverse magnetization decay of water protons tends to exhibit multi-exponential behaviors, due to the multicomponent water protons with different T_2 values, which can be used to directly evaluate the mobility of water molecules, as well as to indirectly probe the changes in polymer chain structure due to water-polymer interactions that affect the translation and rotation motions of water molecules (Okada et al., 2002; Zhang et al., 2004). The T_2 value not only depends on their intrinsic relaxation behavior, but also the exchange process of water protons due to diffusional interchange of water protons between free and bound water molecules, and chemical interexchange between water and exchangeable protons of polymer (–OH, –NH, –COOH groups) (Hills, Takacs, & Belton, 1989; Ibbett, Wortmann, Varga, & Schuster, 2014). According to Ritota et al. (2008), Hills, Wright, and Belton (1989) and Hills et al. (1989), T2 values of water, interpreted on the basis of the diffusive and chemical exchange models, can provide valuable morphological information ranging from molecular to macroscopic scales in biopolymer systems. Researchers have exploited LF NMR combined with proton exchange models to study the morphological properties of Mozzarella di Bufala Campana cheese, rice starch, wheat starch, and bovine serum albumin systems (Belotti, Martinelli, Gianferri, & Brosio, 2010; Gianferri et al., 2007; Le Botlan, Rugraff, Martin, & Colonna, 1998; Ritota et al., 2008).

In this study, the first objective was to investigate the T_2 relaxation spectra of pullulan film-forming solutions dried at 50 °C. The second objective was to elucidate the morphology of pullulan samples during drying by using the diffusive and chemical exchange models.

2. Materials and methods

2.1. Materials

Pullulan (TCI-P0978) was purchased from TCI Chemicals Lab. Inc. (Tokyo, Japan). Redistilled water was used in the preparation of all solutions.

2.2. Structural and characterization of pullulan

The molecular weight distributions of pullulan and alginate were determined using the high-performance size exclusion chromatography system equipped with multi-laser scattering and refractive index detectors (HPSEC-MALLS-RI) (Wyatt Technology Corp., Santa Barbara, USA), as described by Lazaridou, Biliaderis, Roukas, and Izydorczyk (2002). Chromatography was performed at room temperature. The mobile phase consisted of a 0.15 M $NaNO_3$ solution containing 0.02% NaN_3 (vacuum-filtered through a 5-µm filter) at a flow rate of 1.3 mL/min. The HPSEC column was PL aquagel-OH MIXED-M (7.5 × 300 mm, bead diameter: 8 µm, Agilent Technologies Co. Ltd, Beijing, China) analytical M_w range from 10^3 to $5 × 10^5$ g/mol based on Dextran T-40 (Pharmacia Biotech, Uppsala, Sweden). The weight-average molar mass (M_w), polydispersity index (M_w/M_n) and radius of gyration (R_g) for pullulan were determined to be $2.698 ± 0.002 × 10^5$ g/mol, $1.706 ± 0.03$, and $35.1 ± 0.002$ nm, respectively.

2.3. Samples preparation

A 4 g of pullulan powder was dissolved in 100 mL of redistilled water, mixed for 3 h at 1300 rpm using a magnetic stirrer (DF-101B, Yueqing, Zhejiang, China) to form film-forming solutions. The film-forming solutions were deaerated under vacuum with the aid of a vacuum pump (SHZ-D(III), Gongyi City Yuhua Instruments Co. Ltd., China).

2.4. NMR measurements

The pullulan film-forming solutions (approximately 20 g) were carefully transferred to 15 mm diameter NMR glass tubes using a syringe to ensuring that none of solutions were deposited on the tube wall. All the tubes were dried in an environmental chamber (PQX-300A, Ningbo Southeast Instrument Company, Ningbo, China) at 50 °C and 55% RH. The resulting samples were then scanned by a Niumag Pulsed NMR analyzer (NMI20, Niumag Corporation, Shanghai, China) at predetermined time intervals as the film-forming solutions underwent drying. The analyzer was operated at a resonance frequency of 21.12 MHz at 32 °C. Same volume of redistilled water during drying was also measured by the NMR analyzer as a reference.

T_2 values of pullulan solutions during drying were measured using the Carr-Purcell-Meiboom-Gill (CPMG) sequence. The T_2 measurements were made with a τ-value (time between 90° and 180° pulse) of 500 µs. The maximum point of every second echo was accumulated using a 90° pulse of 17 µs and a 180° pulse of 35 µs. Data from 10,000 echoes were acquired as 64 scan repetitions, and the repetition time between subsequent scans was 3 s. All analysis was done in triplicate and coefficients of variation were less than 10%. The T_2 relaxation time spectrum was created following Eq. (1):

$$M(t) = \sum_{i=1}^{N} P_i \exp\left(-\frac{t}{T_{2i}}\right) \tag{1}$$

where P_i was the amplitude size of the ith component; t is the decay time; and T_{2i} was the transverse relaxation time of ith relaxation component.

2.5. Data analysis

All experiments were conducted in triplicate. Analysis of variance (ANOVA) procedure was used to analyze data, using SAS software (Statistical Analysis System Inst. Inc., Cary, NC, USA).

3. Results and discussion

3.1. T_2 relaxation spectra of water during drying

Changes in T_2 value for redistilled water as a function of drying time are presented in Fig. 1, showing one peak at around 2154 ms that decreased in area as drying time increased. Transverse magnetization decay curves showed a single-exponential behavior (Fig. 1 inset) due to homogeneity of the test water.

3.2. T_2 relaxation spectra of pullulan solutions during drying

Fig. 2 displays the T_2 spectra of pullulan film-forming solutions as a function of drying time. At the beginning of the drying process (0 min), two peaks were observed at around 32.77 and 2149 ms (Fig. 2a), which can be assigned to the free water in pullulan solutions (T_{2f}) and moderately bound water in the fully swollen pullulan chains (T_{2b}), respectively. As the drying process continued up to 1200 min, an additional peak appeared in the T_2 spectra at around
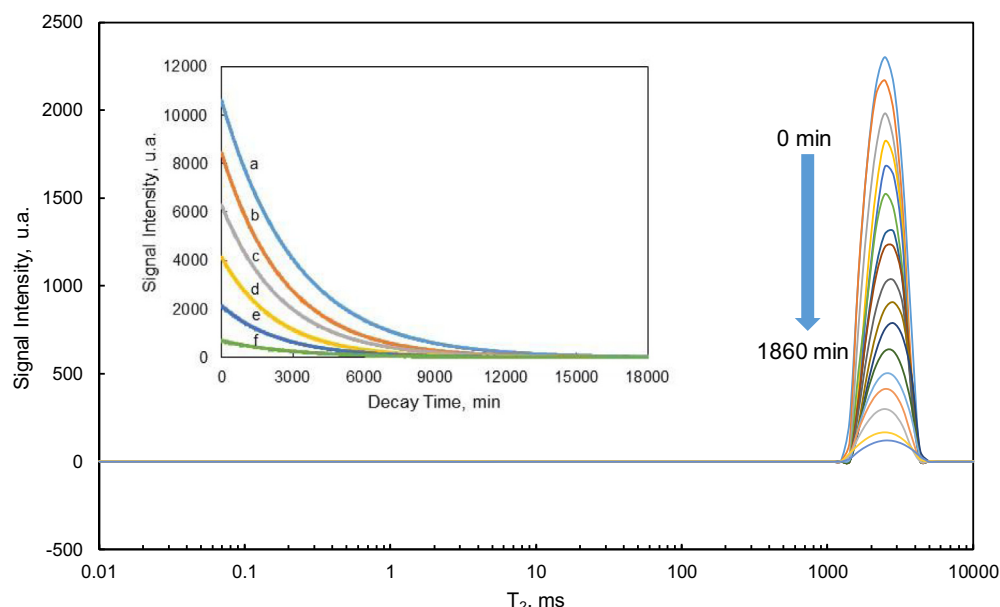
Fig. 1. T_2 relaxation spectra for redistilled water as a function of drying time. Inset is the transverse magnetization decay curves for redistilled water, measured by CPMG sequence, at different drying time: (a) 0 min; (b) 480 min; (c) 840 min; (d) 1200 min; (e) 1560 min; and (f) 1860 min.

3.51 ms (Fig. 2d). This peak could be ascribed to the tightly bound water molecules in the entanglement zones of pullulan chains (T_{2t}) that interacted directly with the -OH groups of pullulan. Similar assignments of water molecules were reported in agarose gels and Mozzarella di Bufala Campana cheese (Belton, Hills, & Raimbaud, 1988; Gianferri et al., 2007).

Contour plots of T_2 spectra for pullulan film-forming solutions as a function of drying time are presented in Fig. 3. As shown in Fig. 3b, the T_{2f} values continuously decreased and eventually disappeared beyond 1560 min, after which, a new peak was observed as the drying process progressed to 1860 min (Fig. 3b). These observations suggested that free water was evaporated after 1560 min, followed by the formation of water cluster in the entangled pullulan chains network as the water content significantly decreased. At the end of drying process (1920 min), when the pullulan films solidified, a contour peak appeared at around 44.47 ms (Fig. 3d), which could be attributable to the water molecules that were loosely bound to the neighboring bound water, as evidenced by its significantly lower magnitude than the T_2 values of water cluster. The existence of tightly bound, moderately bound, and loosely bound water species in pullulan films is consistent with the ATR-FTIR analyses from our previous study (Xiao, Lim, & Tong, 2012).

Fig. 4 presents the peak values of T_2 spectra for pullulan film-forming solutions as functions of drying time and pullulan concentration. As shown, the drying process of pullulan solutions could be divided to three stages, consistent with a gravimetric analysis from our previous study (Xiao et al., 2015). During the first stage (up to 1080 min), as the pullulan concentration increased from 4 to 9.8% (w/w), the values of T_{2b} and T_{2f} were observed at about 32.77–31.45 ms and 2154–1417 ms, respectively. Minimal changes in T_{2b} values were observed during this stage of drying ($p > 0.05$), probably because pullulan chains were flexible and relatively far away each other, i.e., limited chain entanglement (Fig. 5a). This speculation is consistent with our previous studies that pullulan solution at low concentration from 4 to 10% (w/w) exhibited Newtonian flow behavior at lower polymer concentration (Xiao et al., 2012, 2015). By contrast, T_{2f} continuously shifted towards lower relaxation times (from 2145 to 1417 ms) during the first 1080 min of drying time, suggesting a loss of mobility for free water had occurred as the pullulan concentration progressively increased. Similar trend was observed by the contour plots of T_2 spectra for pullulan solutions during drying (Fig. 3a and c).

Towards the second stage of drying process, the appearance of three T_2 peaks in Fig. 2d-f indicates that a multi-exponential relaxation behavior prevailed when the pullulan samples were dried beyond 1080 min. As shown in Fig. 3, both T_{2b} and T_{2f} values progressively decreased (28.48–21.54 ms and 1072–705 ms, respectively, $p < 0.05$). This could be attributed to the formation of transient network by pullulan molecular chains. During this drying stage, as the pullulan concentration increased, pullulan chains began to overlap each other to form a loose network, resulting in concomitant restriction in motion of water molecules (Fig. 5b).

During the third stage of drying process, as pullulan concentration increased to 30.8% (w/w), free water in pullulan samples was evaporated. As a result, water clusters were spatially constrained within a tight network formed by hyper-entangled pullulan chains, then disappeared as the pullulan film solidified (Fig. 5c). For T_{2t} value, it is noteworthy that a decreasing trend was observed after 1440 min of drying time. This observation could be attributed to the conformational transitions and Inter-/intramolecular association between the pullulan chains (Xiao et al., 2014). At the last stage of this drying process, transition of the polymer from less- to more-ordered conformation led to fewer –OH groups available to exchange with water protons. Similar phenomena have been reported in other polymer systems, such as during the aggregation of bovine serum albumin and gelation of carrageenan (Hills et al., 1989; Zhang et al., 2004).

3.3. Diffusive and chemical exchange model

As discussed in Section 3.2, only T_{2b} and T_{2f} values could be determined at the first drying stage. It has been suggested in the literature that the interaction between the bound water and a polymer is determined by the exchange of free water to the water molecules which are directly bound to the hydrophilic site of polymer chains. Accordingly, it is reasonable to hypothesize that T_{2b} is controlled by diffusive exchange between free water and the
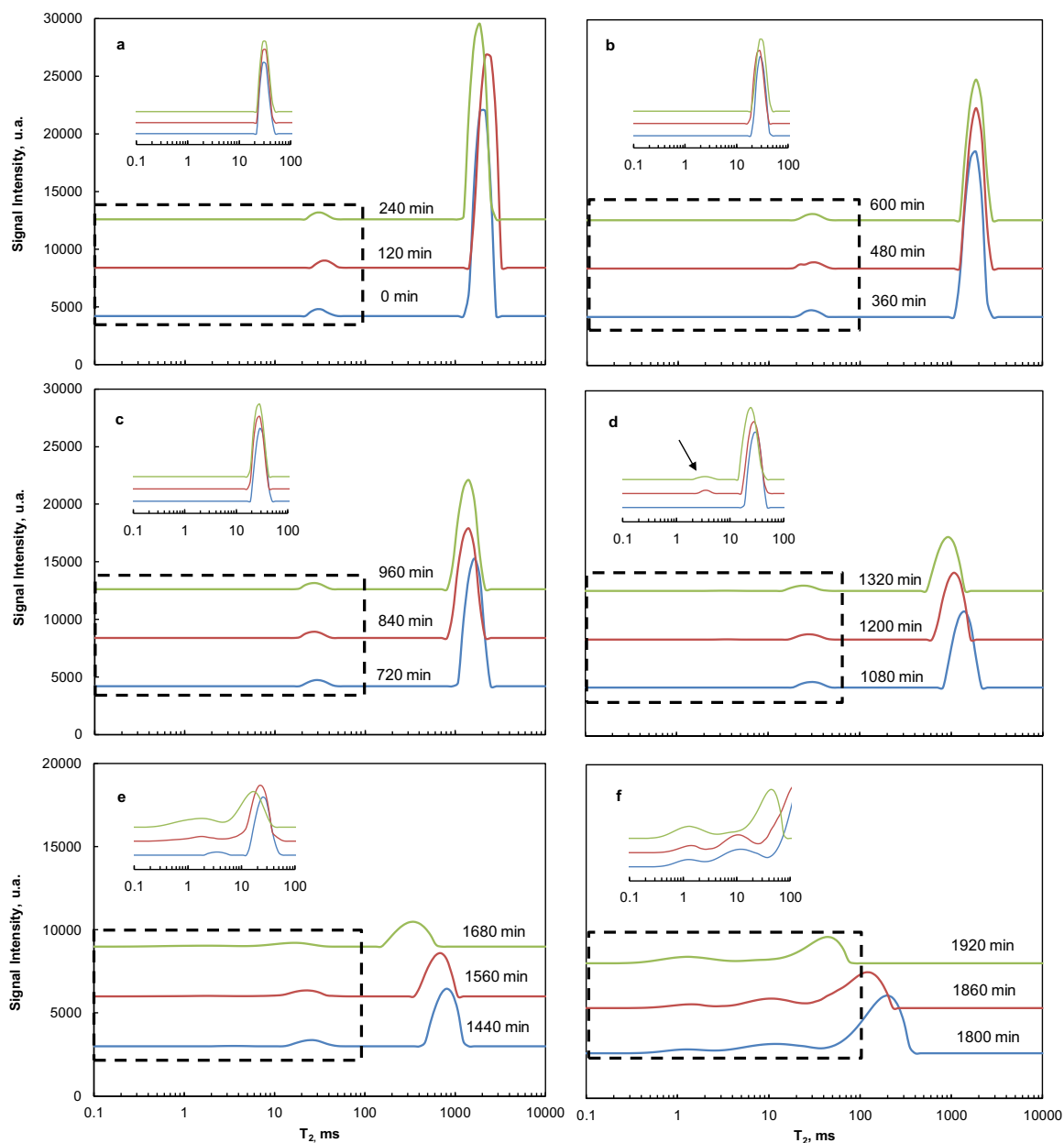
Fig. 2. T_2 relaxation spectra of pullulan film-forming solutions as a function of drying time. Inset is the enlarged spectra range from 0.1 to 100 ms.

tightly bound water on the binding site of polymer (Hills et al., 1989). However, for pullulan, the constant T_{2b} values observed in this study suggested that the moderately bound water was not affected by diffusion exchange between free water and the tightly bound water on the binding site of pullulan during the initial drying process, due to the low concentration of pullulan solutions. Similar results have been reported for dilute dextran, laminaran, and sodium κ-carrageenan solutions (Hills, Cano, & Belton, 1991). As the drying process continued, the network formed by overlapping pullulan chains, as well as the additional T_{2t} values observed as pullulan concentration increased from 11.8 to 98.6% (w/w), indicates the existence of spatial heterogeneity within the drying solutions during the second and third drying stages due to the multi-exponential relaxation behavior for water protons. Moreover, observed T_{2t} value is related to both intrinsic relaxation behavior and the chemical interexchange between water and exchangeable protons of pullulan (Hills et al., 1989; Ibbett et al.,

2014). Therefore, the diffusive and chemical exchange processes of water molecules were expected in pullulan samples at the second and third stages of drying process.

According to Belton et al. (1988), the transverse relaxation behavior was related to the distance scale in heterogeneous systems, dictated by the diffusive exchange of water molecules confined within the spatially heterogeneous regions with the bound water. On the basis of this hypothesis, when the distance between these heterogeneous domains is small, complete diffusive averaging of water molecules will dominate. As a result, the relaxation of water will be in the fast exchange relaxation regime. Conversely, if the distance is large diffusive exchange will be limited, i.e., the relaxation of water molecules will be in the diffusion exchange regime. In heterogeneous systems, researchers have characterized the relaxation properties tightly bound water and bound water as being in the slow-diffusion exchange regime (Belton & Hills, 1987;
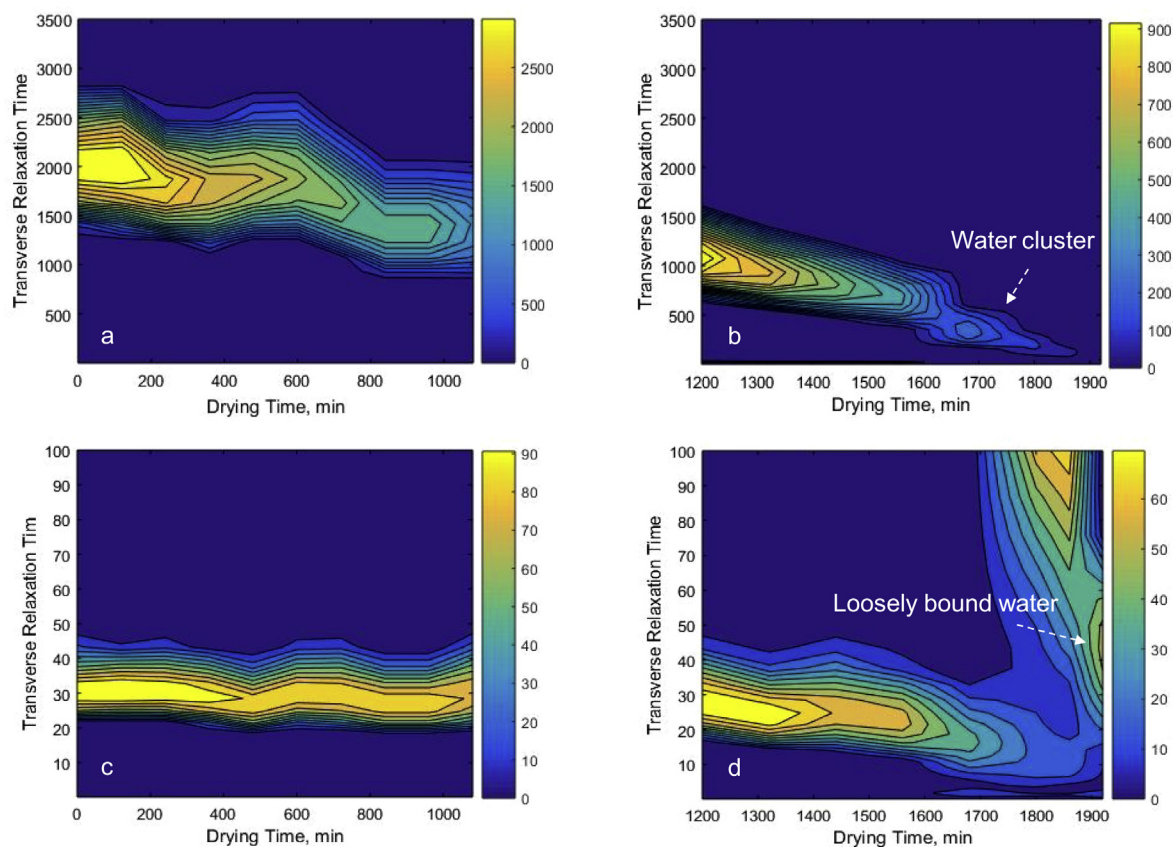
Fig. 3. Contour plots of T_2 spectra for pullulan film-forming solutions as a function of drying time (a) from 0 to 1080 min; (b) from 1200 to 1920 min; (c) enlarged (a) at the T_2 range from 0.1 to 100 ms; and (d) enlarged (b) at the T_2 range from 0.1 to 100 ms.
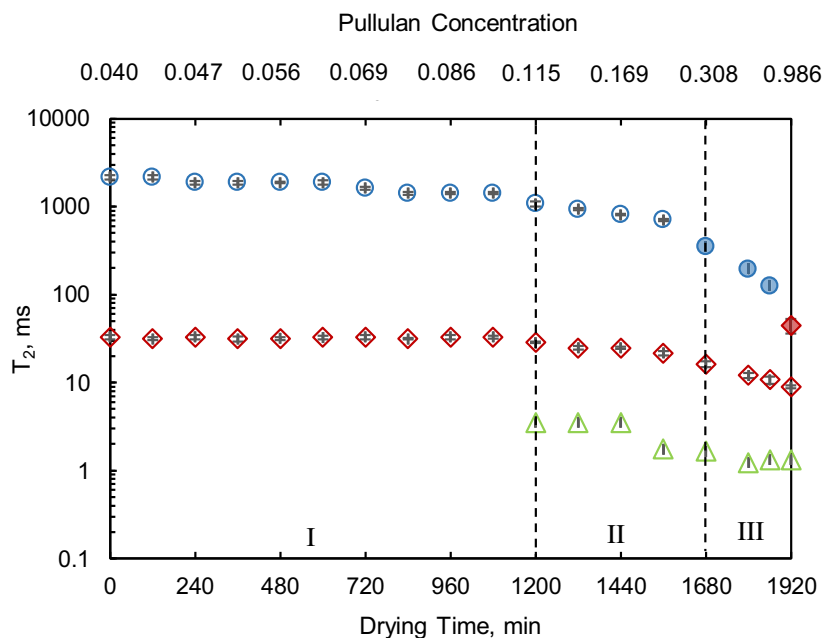

Fig. 4. The peak values of T_2 spectra for pullulan film-forming solutions as a function of drying time and pullulan concentration. ($\triangle$) Tightly bound water in entanglement zones; ($\diamond$) bound water; ($\blacklozenge$) loosely bound water; ($\bigcirc$) free water; and ($\bullet$) water cluster.

Belton et al., 1988). Thus, the minimum dimension of heterogeneity is defined as (Belton & Hills, 1987; Hills, Takacs, & Belton, 1990).

$$\frac{D}{a^2} = \left| \frac{1}{T_{2t}} - \frac{1}{T_{2b}} \right| \qquad (2)$$
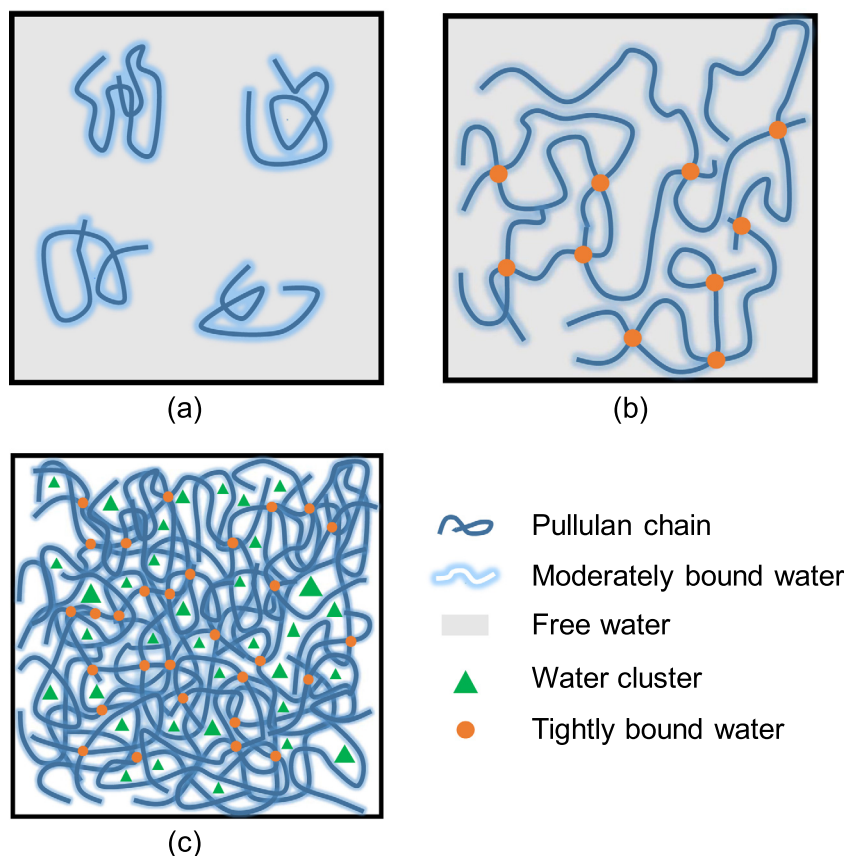
Fig. 5. A schematic illustrating the distribution of water molecules in pullulan film-forming solutions as the drying process progressed. (a) At the first stage; (b) at the second stage; (c) at the third stage of drying process.

where a is the characteristic dimension of the spatial heterogeneity, D is the water self-diffusion coefficient (2.023×10^{-9} m^2 s^{-1}) at 50 °C, T_{2t} and T_{2b} are the relaxation time of tightly bound water, and bound water, respectively.

Under diffusion-limited relaxation regime, the bound water could act as a relaxation sink when water relaxation on the active binding sites of biopolymer is faster than water diffusion to the binding sites. The maximum diffusion distance scale could be estimated by the Eq. (3) (Belton et al., 1988; Gianferri et al., 2007):

$$\frac{1}{T_{2b}} = \frac{1}{T_{2w}} + \frac{\pi^2 D}{a^2} \tag{3}$$

where T_{2w} is water protons intrinsic relaxation time (2.14 s).

From Eqs. (2) and (3), the estimated dimensions of the spatial heterogeneity for pullulan network as a function of drying time were calculated and presented in Fig. 6a. At the beginning of the second stage of drying (at 1200 min), the estimated dimension range of pullulan network was about 7.69–32.66 μm. As the drying time continued to 1860 min, the dimension range of pullulan network gradually decreased to 4.86–19.94 μm due to the formation of entanglement network by the hyper-entangled pullulan chains with drying. Additionally, it is noteworthy that the rough estimated dimension of pure pullulan films was about 4.73–18.14 μm, based on Eqs. (2) and (3).

For tightly bound waters in the entanglement zones of pullulan networks, their oxygen atoms interacted with hydrogens protons of pullulan molecules via hydrogen bonding. Thus, the observed T_{2t} value is dominated by fast chemical exchange between water and hydroxyl protons of pullulan molecules, due to the shorter distance between tightly bounded water and pullulan, according to Eq. (4):

$$\frac{1}{T_{2t}} = \frac{1}{T_{2w}} + \frac{P_{exc}}{T_{2exc} + k_{exc}^{-1}} \tag{4}$$

where T_{2exc} is the intrinsic relaxation time of exchangeable protons of the pullulan chain, which cannot be measured directly and is usually deduced from relaxation time of inert protons on the pullulan. The T_{2exc} value has been estimated to be about 17 μs by Okada et al. (2002). P_{exc} is the molar fraction of exchangeable protons on pullulan, and k_{exc} is the rate of chemical exchange between water and pullulan.

As shown in Fig. 6b, the k_{exc} values remained constant at about 0.227×10^3 s^{-1} with drying time from 1200 to 1440 min, whereas a significantly increase up to 5.817×10^3 s^{-1} was observed at 1800 min. This could be attributed to the changes in conformational and macromolecular orders for pullulan during drying. At the later stage of the drying process, the formation of more-ordered pullulan chain structure, as well as increased pullulan chain-chain interaction, accelerated the chemical exchange rate between water and pullulan molecules.

4. Conclusion

Transverse relaxation time of pullulan film-forming solutions dried at 50 °C were investigated by low-field nuclear magnetic resonance. During the first stage of the drying process (up to 1080 min), two T_2 values were observed at about 32.77–31.45 and 2154–1417 ms, respectively. The longest T_2 value could be assigned to the free water in pullulan solutions, whereas the shorter value could be attributed to bound water with the fully swollen pullulan chains. As the drying process continued, an additional T_2 value appeared with a relaxation time of around 3.51 ms,
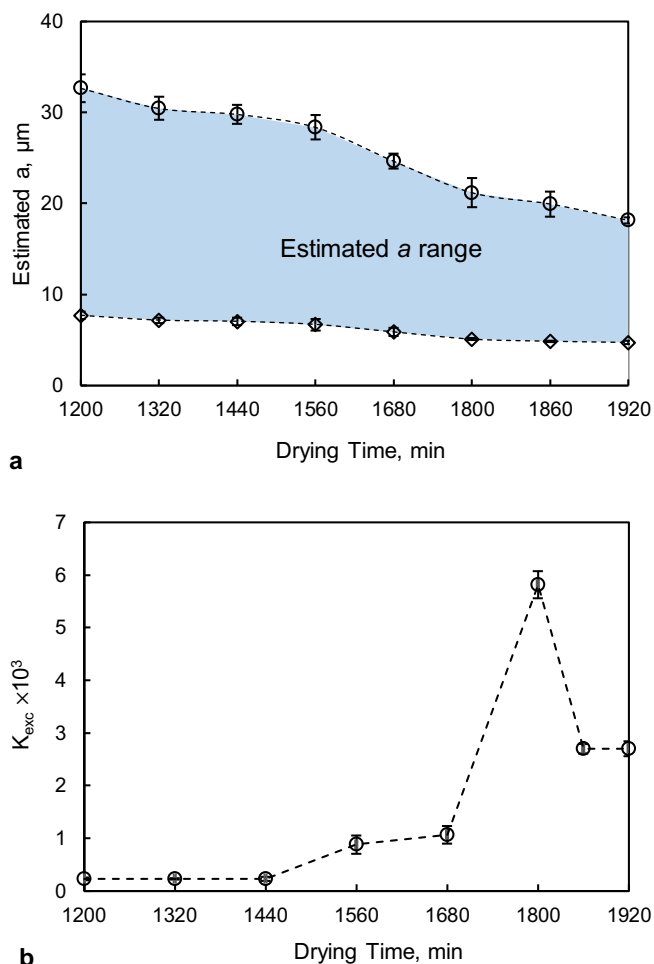
Fig. 6. (a) Estimated dimension of spatial heterogeneity for the pullulan network. The upper and lower lines represent maximum and minimal a values, respectively. (b) Chemical exchange rate of pullulan during drying beyond 1080 min.

which was related to the tightly bound water in the entanglement zones of pullulan chains. Beyond 1560 min, as pullulan concentration increased to 57.7% (w/w), free water in the pullulan matrix was evaporated. As a result, water clusters were spatially constrained within the compacted entanglement network formed by hyper-entangled pullulan chains. The water clusters disappeared upon further drying as the pullulan film solidified. Base on the diffusive and chemical exchange model, the estimated dimension range of pullulan network decreased from 7.69–32.66 to 4.73–18.14 μm as the drying time increased from 1200 to 1920 min. Furthermore, k_{exc} values remained constant about $0.227 \times 10^3 \ s^{-1}$ with increasing drying time from 1200 to 1440 min, whereas a significantly increase in k_{exc} value up to $5.817 \times 10^3 \ s^{-1}$ was observed at 1800 min. The knowledge obtained from this study not only provides an effective method for real-time monitoring water dynamics during drying process of film-forming solutions, but also helps to predict morphological information of polymer network as the edible films being solidified.

Acknowledgments

References

Belotti, M., Martinelli, A., Gianferri, R., & Brosio, E. (2010). A proton NMR relaxation study of water dynamics in bovine serum albumin nanoparticles. *Physical Chemistry Chemical Physics, 12*(2), 516–522.

Belton, P. S., & Hills, B. (1987). The effects of diffusive exchange in heterogeneous systems on NMR line shapes and relaxation processes. *Molecular Physics, 61*(4), 999–1018.

Belton, P., Hills, B., & Raimbaud, E. (1988). The effects of morphology and exchange on proton NMR relaxation in agarose gels. *Molecular Physics, 63*(5), 825–842.

Chen, L., Tian, Y., Tong, Q., Zhang, Z., & Jin, Z. (2017). Effect of pullulan on the water distribution, microstructure and textural properties of rice starch gels during cold storage. *Food Chemistry, 214*, 702–709.

Cheng, K.-C., Demirci, A., & Catchmark, J. M. (2011). Pullulan: Biosynthesis, production, and applications. *Applied Microbiology and Biotechnology, 92*(1), 29.

Foster, R. J., Damion, R. A., Baboolal, T. G., Smye, S. W., & Ries, M. E. (2016). A nuclear magnetic resonance study of water in aggrecan solutions. *Royal Society Open Science, 3*(3).

Ghi, P. Y., Hill, D. J. T., & Whittaker, A. K. (2002). H NMR study of the states of water in equilibrium poly(HEMA-co-THFMA) hydrogels. *Biomacromolecules, 3*(5), 991–997.

Ghoshal, S., Denner, P., Stapf, S., & Mattea, C. (2012). Study of the formation of poly (vinyl alcohol) films. *Macromolecules, 45*(4), 1913–1923.

Ghoshal, S., Mattea, C., Denner, P., & Stapf, S. (2010). Heterogeneities in gelatin film formation using single-sided NMR. *The Journal of Physical Chemistry B, 114*(49), 16356–16363.

Gianferri, R., D'Aiuto, V., Curini, R., Delfini, M., & Brosio, E. (2007). Proton NMR transverse relaxation measurements to study water dynamic states and age-related changes in Mozzarella di Bufala Campana cheese. *Food Chemistry, 105* (2), 720–726.

Hills, B., Cano, C., & Belton, P. (1991). Proton NMR relaxation studies of aqueous polysaccharide systems. *Macromolecules, 24*(10), 2944–2950.

Hills, B., Takacs, S., & Belton, P. (1989). The effects of proteins on the proton NMR transverse relaxation time of water: II. Protein aggregation. *Molecular Physics, 67*(4), 919–937.

Hills, B., Takacs, S., & Belton, P. (1990). A new interpretation of proton NMR relaxation time measurements of water in food. *Food Chemistry, 37*(2), 95–111.

Hills, B., Wright, K., & Belton, P. (1989). Proton NMR studies of chemical and diffusive exchange in carbohydrate systems. *Molecular Physics, 67*(6), 1309–1326.

Ibbett, R. N., Schuster, K. C., & Fasching, M. (2008). The study of water behaviour in regenerated cellulosic fibres by low-resolution proton NMR. *Polymer, 49*(23), 5013–5022.

Ibbett, R., Wortmann, F., Varga, K., & Schuster, K. C. (2014). A morphological interpretation of water chemical exchange and mobility in cellulose materials derived from proton NMR T2 relaxation. *Cellulose, 21*(1), 139–152.

Lazaridou, A., Biliaderis, C. G., Roukas, T., & Izydorczyk, M. (2002). Production and characterization of pullulan from beet molasses using a nonpigmented strain of Aureobasidium pullulans in batch culture. *Applied Biochemistry and Biotechnology, 97*(1), 1–22.

Le Botlan, D., Rugraff, Y., Martin, C., & Colonna, P. (1998). Quantitative determination of bound water in wheat starch by time domain NMR spectroscopy. *Carbohydrate Research, 308*(1–2), 29–36.

Okada, R., Matsukawa, S., & Watanabe, T. (2002). Hydration structure and dynamics in pullulan aqueous solution based on 1H NMR relaxation time. *Journal of Molecular Structure, 602–603*, 473–483.

Ritota, M., Gianferri, R., Bucci, R., & Brosio, E. (2008). Proton NMR relaxation study of swelling and gelatinisation process in rice starch–water samples. *Food Chemistry, 110*(1), 14–22.

Singh, R. S., Saini, G. K., & Kennedy, J. F. (2008). Pullulan: Microbial sources, production and applications. *Carbohydrate Polymers, 73*(4), 515–531.

Spěváček, J., Hanyková, L., & Labuta, J. (2011). Behavior of water during temperature-induced phase separation in poly(vinyl methyl ether) aqueous solutions. NMR and optical microscopy study. *Macromolecules, 44*(7), 2149–2153.

Tang, H. R., Godward, J., & Hills, B. (2000). The distribution of water in native starch granules—A multinuclear NMR study. *Carbohydrate Polymers, 43*(4), 375–387.

Xiao, Q., Lim, L.-T., & Tong, Q. (2012). Properties of pullulan-based blend films as affected by alginate content and relative humidity. *Carbohydrate Polymers, 87* (1), 227–234.

Xiao, Q., Tong, Q., & Lim, L.-T. (2012). Pullulan-sodium alginate based edible films: Rheological properties of film forming solutions. *Carbohydrate Polymers, 87*(2), 1689–1695.

Xiao, Q., Tong, Q., & Lim, L.-T. (2014). Drying process of pullulan edible films forming solutions studied by ATR-FTIR with two-dimensional correlation spectroscopy. *Food Chemistry, 150*, 267–273.

Xiao, Q., Tong, Q., Zhou, Y., & Deng, F. (2015). Rheological properties of pullulan-sodium alginate based solutions during film formation. *Carbohydrate Polymers, 130*, 49–56.

Zhang, Q., Matsukawa, S., & Watanabe, T. (2004). Theoretical analysis of water 1H T2 based on chemical exchange and polysaccharide mobility during gelation. *Food Hydrocolloids, 18*(3), 441–449.